

# Hydrothermal Alteration and Mineralization at the Kerr and Deep Kerr Copper-Gold Porphyry Deposits, Northwestern British Columbia (Parts of NTS 104B/08)

S. Rosset, Mineral Deposit Research Unit, University of British Columbia, Vancouver, BC, srosset@eos.ubc.ca

C.J.R. Hart, Mineral Deposit Research Unit, University of British Columbia, Vancouver, BC

Rosset, S. and Hart, C.J.R. (2016): Hydrothermal alteration and mineralization at the Kerr and Deep Kerr copper-gold porphyry deposits, northwestern British Columbia (parts of NTS 104B/08); in Geoscience BC Summary of Activities 2015, Geoscience BC, Report 2016-1, p. 175–184.

## Introduction

Porphyry copper±gold and molybdenum deposits are well represented in British Columbia, traditionally contributing the largest copper reserves and significant resources of molybdenum, and hosting nearly 50% of gold reserves in the province (Panteleyev, 1995). The Quesnel and Stikine terranes of BC host belts of calcalkalic and alkalic porphyry deposits, related to Late Triassic to Middle Jurassic volcanic arcs that accreted to the western margin of North America (Figure 1). Related porphyry copper±gold and molybdenum deposits are largely restricted to a 15 m.y. epoch from the Late Triassic to the Early Jurassic, and are a result of slab subduction (Logan and Mihalynuk, 2014).

These Mesozoic deposits are difficult exploration targets, with complex alteration and metal-zoning patterns. Post-emplacement deformation further complicates improved understanding of these deposits and subsequent exploration decision making. The character, distribution and intensity of hydrothermal-alteration–mineral assemblages in porphyry deposits reflect the nature and distribution of economic metals. Research into the complexity of alteration–mineral assemblages and their zoning can better define the deposit and the relationships between alteration and mineralization. This is particularly important since hostrocks are highly altered and can be difficult to identify. Characterization of the chemical composition of hydrothermal-alteration assemblages, and isotopic composition of sulphides and sulphates, provide data on hydrothermal fluids, such as pH, temperature and oxidation state, that can provide exploration vectors toward mineralization (Wilson et al., 2007; Jimenez, 2011; Cohen; 2012; Dilles, 2012).

The Kerr and Deep Kerr deposits are part of the Kerr-Sulphurets-Mitchell (KSM) property, which represents one of the largest undeveloped porphyry systems in the world.

**Keywords:** Stikine terrane, Stuhini Group, Hazelton Group, Texas Creek Plutonic Suite, porphyry, copper, gold, molybdenum, hydrothermal alteration, KSM property, Kerr, Deep Kerr

This publication is also available, free of charge, as colour digital files in Adobe Acrobat® PDF format from the Geoscience BC website: <http://www.geosciencebc.com/s/DataReleases.asp>.

A research project jointly initiated by the Mineral Deposit Research Unit at the University of British Columbia and Seabridge Gold Inc., with support from Geoscience BC, will focus on the characterization and evolution of hydrothermal-alteration assemblages and mineralization to provide a

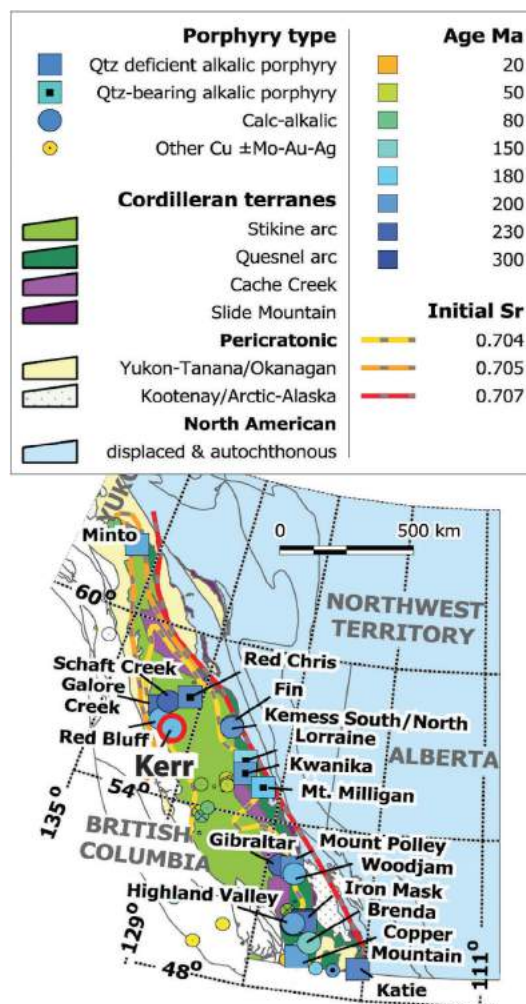


**Figure 1.** Porphyry deposits within the Canadian Cordillera, and location of the Kerr deposit in northwestern British Columbia (modified from Logan and Mihalynuk, 2014). Deposits are colour coded according to age, with Late Triassic to Early Jurassic porphyry deposits in blue; initial Sr isopleths are those of Mesozoic plutons (Logan and Mihalynuk, 2014).

better understanding of their correlation. This will be achieved through 1) detailed petrographic analysis and macroscopic observations; 2) shortwave infrared spectroscopy (SWIR); 3) major- and minor-element geochemistry and verification of SWIR results through scanning electron microscopy (SEM), X-ray powder diffraction (XRD), and electron probe micro-analysis (EPMA); and 4) sulphur-isotope analysis of sulphide and sulphate minerals to identify variability with respect to mineralization and alteration-mineral assemblages. This research project aims to contribute to the improvement of exploration tools and geometallurgical decision making, thereby increasing exploration and economic success in British Columbia and similar environments globally.

Fieldwork during 2015 focused on a 2.5 km southeast-trending cross-section across the north-central Kerr and Deep Kerr deposits. Nine drillholes were logged and sampled for a total of over 7000 m, with emphasis on detailed alteration logging and documentation of crosscutting relationships to establish vein paragenesis. More than 1100 chip samples for SWIR analysis were collected, with an additional 152 samples for whole-rock geochemical, petrographic and sulphur-isotope analysis. These observations will form the basis for ongoing petrographic, SWIR, SEM, XRD, EPMA and sulphur-isotope analyses in order to characterize the spatial distribution and evolution of hydrothermal alteration and mineralization.

### Tectonic Setting

British Columbia is composed largely of terranes of exotic crustal fragments that accreted to the ancient North American margin during the Mesozoic era. The Intermontane Belt comprises much of the accreted material along the Canadian Cordillera in British Columbia and is predominantly composed of the Stikine terrane, the Quesnel terrane and the intervening Cache Creek terrane. Porphyry deposits are concentrated within the Stikine and Quesnel terranes, which feature nearly equivalent stratigraphy and Devonian to Early Jurassic evolution (Logan and Mihalynuk, 2014). The KSM property is hosted within the western margin of northern Stikinia, in the Sulphurets district. Porphyry mineralization in this district has been dated between 197 and 190 Ma (Bridge, 1993; Margolis, 1993; Kirkham and Margolis, 1995; Febbo et al., 2015).

### Regional Geology

The Stikine terrane in northwestern British Columbia is composed of island-arc volcano-sedimentary successions that include the Stikine assemblage (Paleozoic), Stuhini Group (Late Triassic) and Hazelton Group (Early Jurassic). These successions are overlain by sedimentary rocks of the Middle Jurassic to Tertiary Bowser Lake and Sustut groups and the Late Cretaceous to Tertiary Sloko Group, and Ter-

tiary<sup>1</sup> Edziza and Spectrum volcanic rocks (Logan et al., 2000). A regional-scale unconformity between the volcano-sedimentary Stuhini Group and overlying volcanic and sedimentary Hazelton Group varies from a sharp angular unconformity to a near disconformity (Kyba, 2014; Nelson and Kyba, 2014). The Early Jurassic Texas Creek Plutonic Suite is comagmatic and coeval with the Lower Hazelton Group, and comprises I-type, calcalkaline intrusive rocks that are cospatial with Hazelton volcanic rocks (Logan et al., 2000). The Mitchell intrusions of the Sulphurets district are considered a subset of the Texas Creek plutons (Kirkham, 1963; Alldrick and Britton, 1991).

### KSM Property Overview and Geology

The KSM property is in northwestern British Columbia, 65 km north of the town of Stewart (Figure 2), and is one of the largest undeveloped gold projects in the world. The claims are 100% owned by Seabridge Gold Inc. The KSM property comprises the Kerr, Deep Kerr, Sulphurets, Mitchell, Iron Cap and Lower Iron Cap deposits, and has an estimated total proven and probable reserve of 38.2 million ounces gold and 9.9 billion pounds copper (Seabridge Gold Inc., 2015a). The Kerr deposit contains an estimated probable reserve of 242 million tonnes grading 0.45% copper and 0.24 g/t gold (containing 2.4 billion lb. copper and 1.9 million oz. gold; Seabridge Gold Inc., 2015a). The Deep Kerr deposit, discovered in 2013, had an initial inferred resource estimate in 2014 and an updated inferred estimate in 2015 of 782 million tonnes grading 0.54% copper and 0.33 g/t gold (containing 9.3 billion lb. copper and 8.2 million oz. gold; Seabridge Gold Inc., 2015b).

The KSM deposits are hosted in volcanic arc-related Triassic to Jurassic volcanic and sedimentary assemblages that were intruded by Early Jurassic diorite, monzonite and quartz syenite intrusions. Volcanic and sedimentary rocks of the Stuhini and Hazelton groups are cut by feldspar porphyry intrusive rocks. These Premier and Sulphurets intrusive rocks are suites within the Mitchell intrusions, and therefore part of the Texas Creek Plutonic Suite. Geochronology and crosscutting relationships suggest that the Sulphurets suite magmatism postdates, and potentially overlaps with Premier suite magmatism (Febbo et al., 2015). The Sulphurets suite fine- to medium-grained diorite to monzonite porphyry hosts porphyry mineralization in the district (Febbo et al., 2015). At the KSM deposits, shallow vein systems and skarns transition to sedimentary- and volcanic-hosted porphyry mineralization in the transitional

---

<sup>1</sup> 'Tertiary' is an historical term. The International Commission on Stratigraphy recommends using 'Paleogene' (comprising the Paleocene to Oligocene epochs) and 'Neogene' (comprising the Miocene and Pliocene epochs). The author used the term 'Tertiary' because it was used in the source material for this paper.

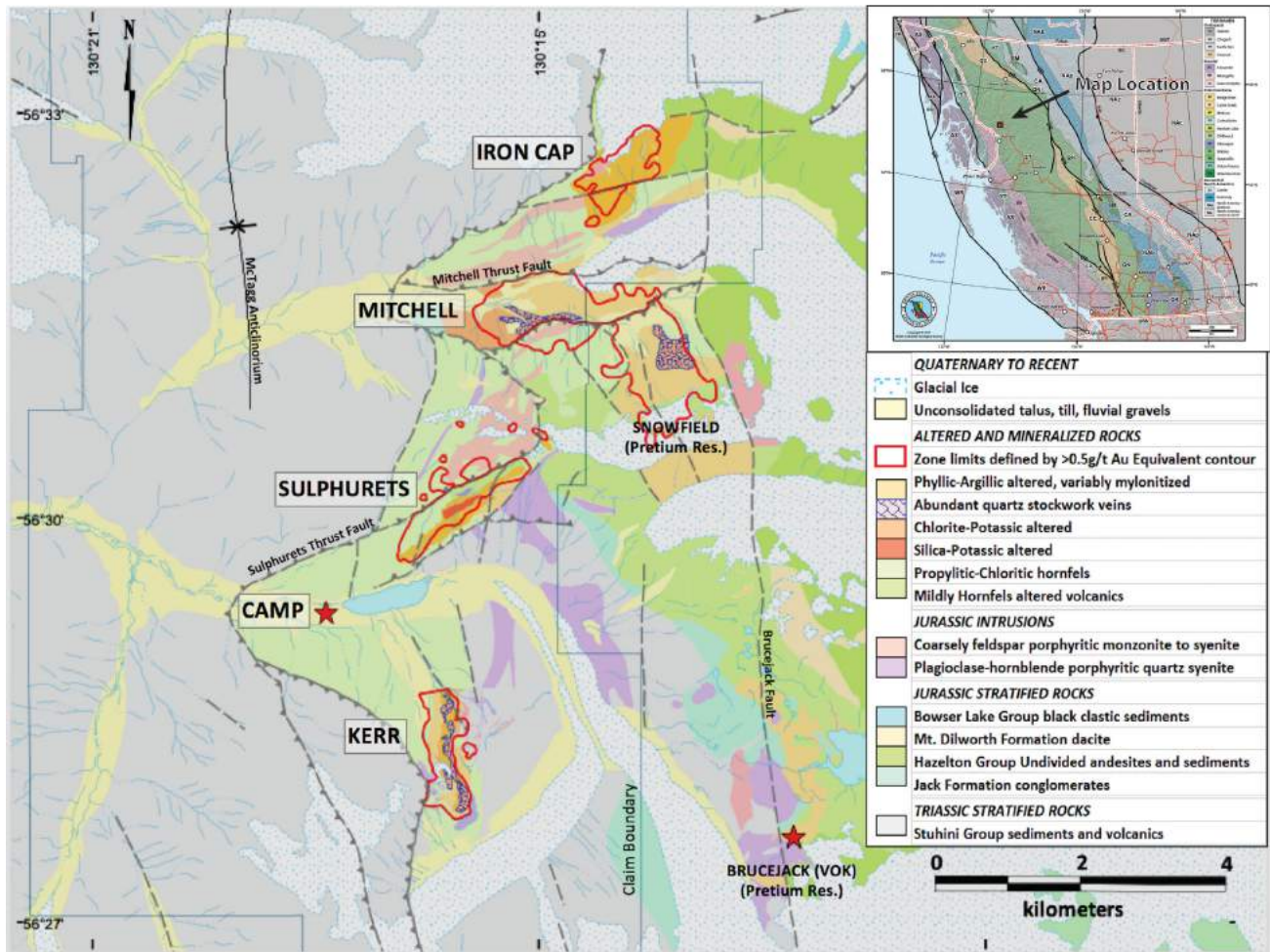


Figure 2. KSM property geology with deposit locations (Seabridge Gold Inc., pers. comm., 2015).

environment, and to intrusion-hosted porphyry mineralization at depth (M. Savell, pers. comm., 2015).

## Kerr and Deep Kerr Deposits

### Deposit Structure and Lithology

The Kerr and Deep Kerr deposits strike north and dip steeply to the west, with the shallower portion of the deposit (upper ~500 m) defined as the Kerr deposit and the newly discovered Deep Kerr deposit underlying the Kerr deposit and open at depth. The steeply dipping 'F2' reverse fault bounds the western margin of the deposit (Febbo et al., 2014). This structure was previously identified as the Sulphurets thrust fault (Bridge, 1993), which has subsequently been mapped to the west as a moderately west-dipping reverse fault (Lewis, 2001; Febbo et al., 2014). Footwall assemblages are represented by sedimentary and volcanoclastic rocks of the Stuhini and Hazelton groups. The F2 fault thrusts Triassic Stuhini Group to Jurassic Hazelton Group basal-fill rocks over younger Hazelton Group rocks in the footwall (Seabridge Gold, pers. comm., 2015). The Kerr deposit is strongly deformed, as pre-exist-

ing structures and intense alteration led to the development of a low-competency zone where Cretaceous compression was focused (Ditson et al., 1995).

The Kerr deposit is largely hosted by assemblages of the Stuhini and Hazelton groups, whereas the Deep Kerr deposit is largely intrusion-hosted. Late Triassic Stuhini Group hostrocks are predominantly siltstone, graphitic shale and mudstone, while Early Jurassic Hazelton Group volcanic and sedimentary hostrocks are represented by sandstone, conglomerate (e.g., Jack Formation; Figure 3a) and lesser volcanic rocks. Synmineralization composite intrusions of porphyritic hornblende-plagioclase±K-feldspar-biotite are the most abundant intrusions at the Kerr and Deep Kerr deposits, and constitute the bulk of the Deep Kerr (Figure 3b). These intrusions crosscut each other, with multiple overprinting intrusive phases, and are highly altered within the deposit, making recognition of primary phases difficult. Early Jurassic K-feldspar-megacrystic porphyry dikes (Figure 3c) are late mineralization and overprinted by epithermal gold-silver mineralization (Bridge, 1993). Postmineralization dikes include Early Ju-

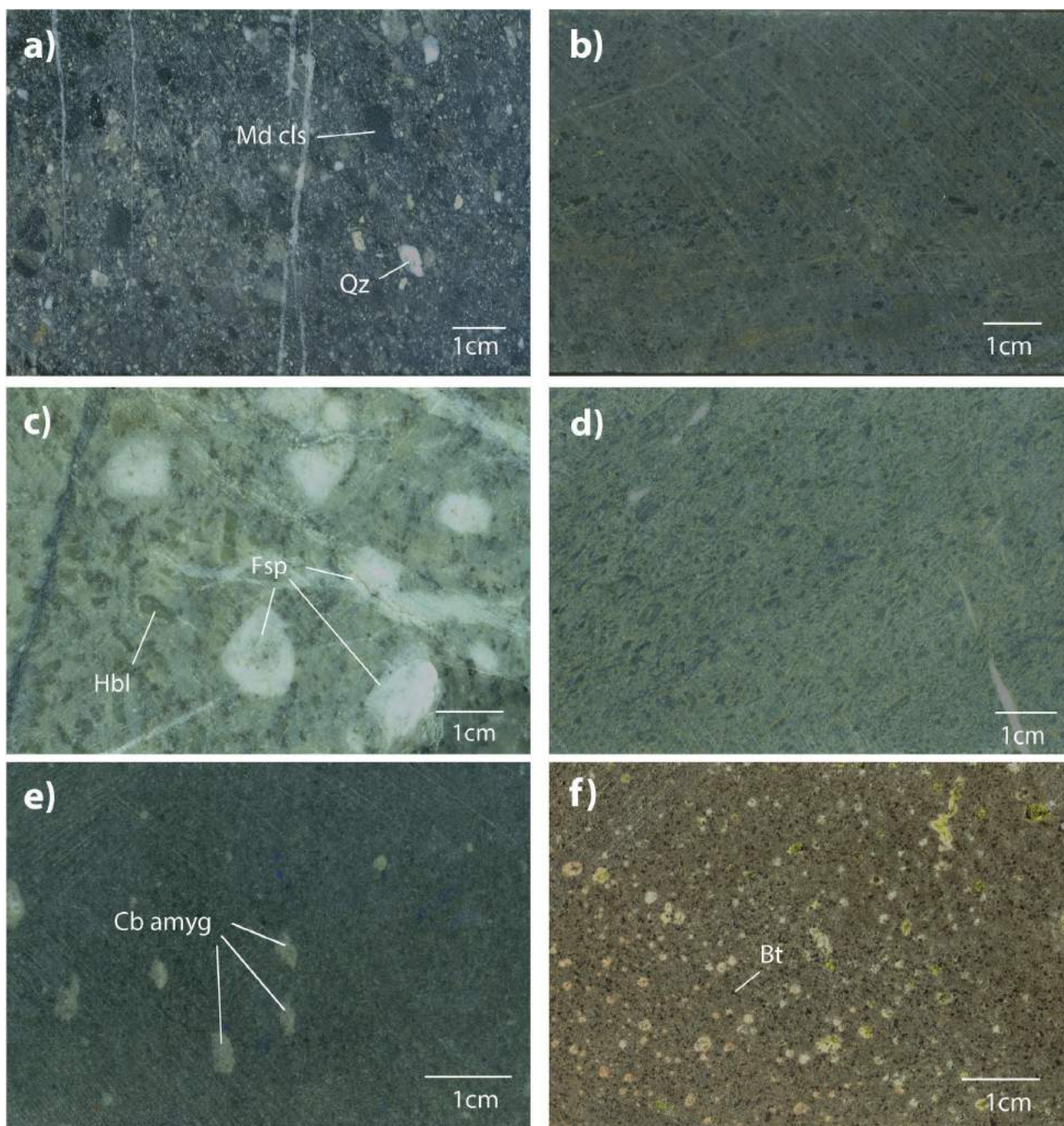


**Figure 3.** Key rock types of the Kerr and Deep Kerr deposits (sample number, drillhole number, depth in metres): **a)** Jack Formation conglomerate, featuring mudstone intraclasts and quartz pebbles (2015-062, K-14-37, 388.95 m); **b)** porphyritic andesite with chlorite/sericite pseudomorphs after hornblende and feldspar (2014-014, K-13-34, 532.6 m); **c)** postmineralization porphyritic diorite dike with chlorite/sericite pseudomorphs after hornblende and feldspar (2015-091, K-13-31, 517.8 m); **d)** K-feldspar–megacrystic porphyry (2015-003, K-12-20, 149.4 m); **e)** aphanitic diorite dike with carbonate amygdules (2014-016, K-13-34, 568.13 m); **f)** postmineralization biotite porphyry dike with feldspar (2015-039, K-13-30, 617.3 m). Abbreviations: Bt, biotite; Cb amyg, carbonate amygdules; Fsp, feldspar; Hbl, hornblende; Md cls, mudstone clasts; Qz, quartz.

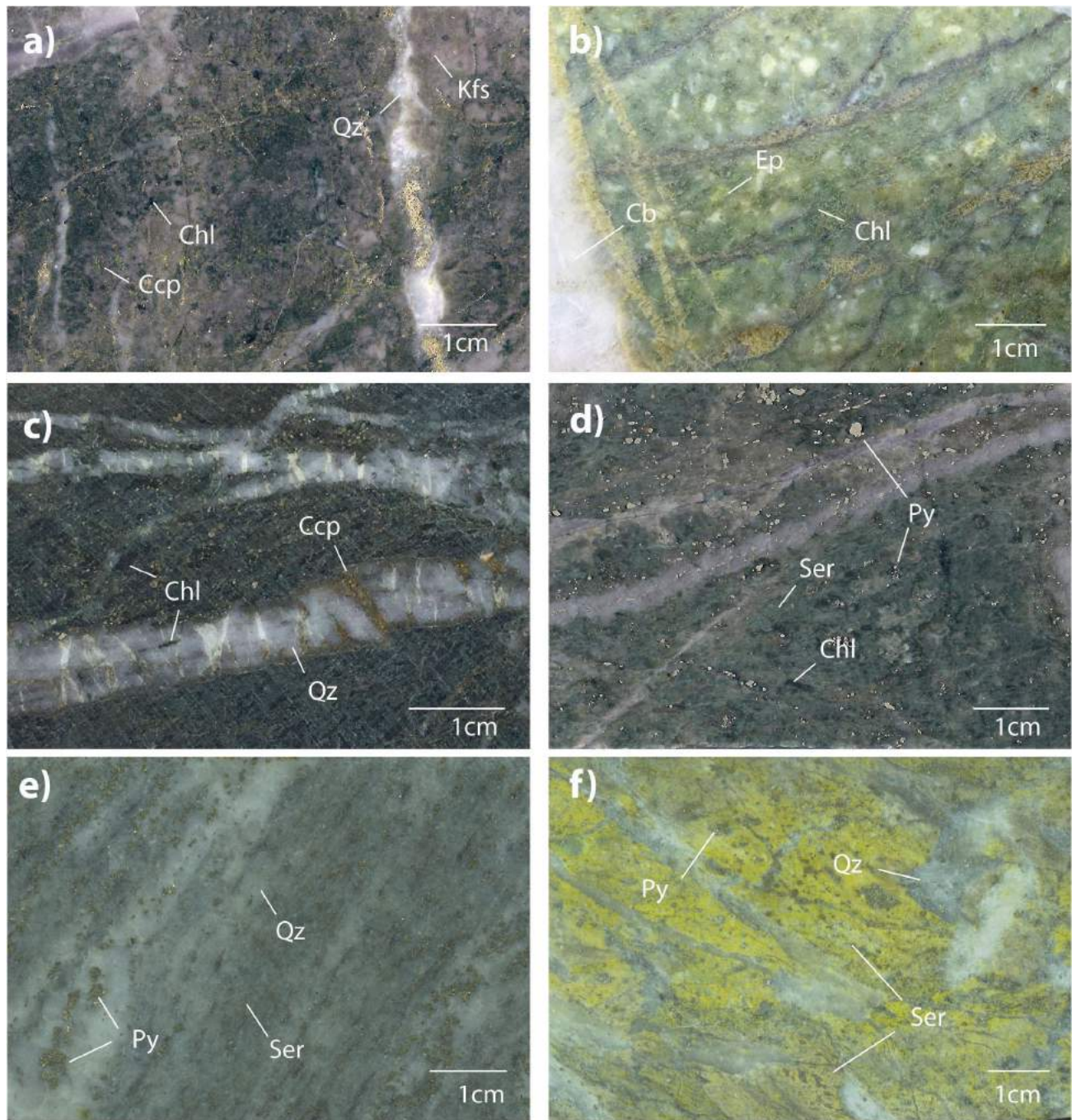


**Figure 4.** Key alteration assemblages of the Kerr and Deep Kerr deposits (sample number, drillhole number, depth in metres): **a)** K-feldspar–chlorite–magnetite alteration with fine-grained chalcopyrite in hornblende-phyric intrusion cut by quartz vein (K-15-49, 1476.6 m); **b)** epidote-chlorite-carbonate alteration within a feldspar-phyric intrusive (K-14-37, 978.4 m); **c)** pervasive chlorite alteration within a hornblende- and feldspar-phyric intrusion, and associated quartz-chalcopyrite-chlorite veining (K-13-31, 594.4 m); **d)** pervasive chlorite-sericite and disseminated pyrite alteration within a hornblende-phyric intrusion (K-14-39, 952.2 m); **e)** pervasive, intense quartz-sericite-pyrite alteration of unknown protolith (2014-023, K-13-31, 1110.9 m); **f)** intense yellow-sericite alteration of a sedimentary protolith (2015-094, K-31-34, 447.7 m). Abbreviations: Cb, carbonate; Ccp, chalcopyrite; Chl, chlorite; Ep, epidote; Kfs, K-feldspar; Py, pyrite; Qz, quartz; Ser, sericite.



rassic porphyritic diorite dikes (Figure 3d) and aphanitic diorite dikes (Figure 3e), and Eocene biotite porphyry kersantitic lamprophyre dikes (Figure 3f; Bridge, 1993).

### Alteration

Alteration at the Kerr deposit is the result of a long-lived, relatively shallow hydrothermal system produced by intrusion of monzonite (Ditson et al., 1995). Alteration at both the Kerr and Deep Kerr deposits (Figures 4, 5) affects sedimentary and volcanic hostrocks, as well as pre- to synmineralization intrusions, with weaker alteration of postmineralization intrusive rocks and very weak alteration of late postmineralization intrusive rocks. Supergene alteration is noted in the shallower Kerr deposit to consist of leached hematite/jarosite, minor native copper and chalcocite/covellite, with extensive hydration of anhydrite to gypsum (Bridge, 1993). This hydration has caused an extensive ‘rubble’ zone in the near-surface environment at Kerr.

Early K-feldspar–chlorite–magnetite alteration (Table 1, Figure 4a) is minor, and preservation is limited to remnant ‘rafts’ in the core of the deposit and at depth in drillhole K-15-49 (Figure 5). Early epidote–chlorite±carbonate alteration (Figure 4b) is minor, and visible at the eastern and western margins of the deposit. K-feldspar–chlorite–magnetite alteration appears to have been largely overprinted by dark green, pervasive chlorite alteration (Figure 4c) with minor remnant magnetite. K-feldspar, chlorite and magnetite alteration are associated with chalcopyrite±bornite mineralization. Pale green, pervasive chlorite–phengite±illite alteration (Figure 4d) occurs within the deposit and is abundant peripheral to the deposit on the west and east, and in shallow hostrocks. This alteration assemblage, as well as the dark chlorite core alteration, are typically overprinted

by a widespread quartz–sericite–pyrite assemblage (Figure 4e), which has an extensive distribution overprinting the core and margins of the deposit. Yellow sericite–pyrite±quartz alteration (Figure 4f) is typically intense and pervasive within minor sedimentary rafts at depth in the deposit (K-13-23A), and in shallow sedimentary hostrocks within the deposit. This alteration was noted by previous workers to be a selective alteration of sedimentary rocks and, due to its peripheral distribution, to contain the lowest metal grades among the alteration assemblages (Ditson et al., 1995).

### Vein Paragenesis

Early magnetite veins (Table 2, Figure 6a) have a limited distribution within the core and at depth at the Kerr and Deep Kerr deposits, and are associated with K-feldspar–chlorite±magnetite alteration. Alteration of magnetite to pyrite may obscure the original extent of these veins. Quartz–chalcopyrite–pyrite veining (Figure 6b, c) is extensive and intimately associated with copper and gold mineralization, forming dense stockworks within the core of the deposit. Extensive quartz–pyrite veining (Figure 6d) overprints earlier veining and is associated with chlorite–sericite and quartz–sericite–pyrite alteration assemblages. These veins are typically planar, with 2–20 mm sericite haloes indicating disequilibrium with surrounding pervasive alteration. Late, white quartz–chalcopyrite–carbonate±chlorite veins (Figure 6e) are distributed throughout the deposit, with higher chalcopyrite contents in higher grade areas suggesting local remobilization. A high-sulphidation overprint is visible as bornite, tennantite/enargite and dickite/pyrophyllite overprinting core stockwork zones (Figure 6f). Anhydrite veining is dominated by late, white to grey veins that overprint quartz–stockwork zones and

**Table 1.** Overview of alteration assemblages at the Kerr and Deep Kerr deposits; vein-type analogues are derived from Sillitoe (2010), modified after Gustafson and Hunt (1975).

Alteration assemblage	Sulphide assemblage	Vein types and analogues <sup>1</sup>	Distribution	Alteration assemblage analogue
K-feldspar–chlorite–magnetite±biotite	Pyrite–chalcopyrite±bornite	Quartz–sulphides (A and B types), magnetite	Limited distribution; occurs at depth (DDH K-15-49), with only remnant rafts within deposit, where magnetite±K-feldspar alteration has been largely overprinted	K-silicate
Epidote–chlorite±carbonate	Pyrite	Quartz–pyrite–epidote	Limited peripheral distribution; occurs at eastern and western margins of deposit	Propylitic
Chlorite±magnetite	Chalcopyrite–pyrite	Quartz–sulphides (A and B types), magnetite associated	Throughout the deposit, with the most intense chlorite alteration within the core of the deposit; potential artifact of K-feldspar–magnetite±biotite alteration	Chlorite
Chlorite–phengite±illite	Pyrite	Quartz–pyrite (D type)	Throughout the deposit, abundant peripheral to core, and overprinting earlier chlorite alteration	Sericite–chlorite
Quartz–sericite	Pyrite	Quartz–pyrite (D type)	Abundant throughout the deposit, commonly overprinting chlorite alteration in the core, and peripheral sericite–chlorite alteration	Phyllic
Yellow sericite±quartz	Pyrite	Quartz–pyrite (D type)	Limited distribution; occurs extensively within sedimentary units peripheral to deposit, and within sedimentary rafts	-

**Table 2.** Overview of vein types at the Kerr and Deep Kerr deposits; vein-type analogues derived from Sillitoe (2010), modified after Gustafson and Hunt (1975). Abbreviation: PCD, porphyry copper deposits.

Mineral-sulphide assemblage	Vein selvage	Description	Alteration assemblage	Distribution	PCD vein-type analogue <sup>1</sup>
Magnetite±pyrite-quartz	None	3–30 mm; sharp, sinuous margins; alter to pyrite	K-feldspar–chlorite–magnetite and chlorite–magnetite	At depth (K-15-49), with minor remnant magnetite within chloritic alteration in the core of the deposit	M type
Quartz–chalcopyrite ±pyrite–bornite–molybdenite	Typically none; Kfs locally (B veins)	Granular to translucent; white to gray/pink; 5–40 mm; A veins sinuous, B veins more planar and may contain sulphide centreline	K-feldspar–chlorite–magnetite and chlorite–magnetite	Common in deposit core, associated with grade and quartz-stockwork veining	A & B types
Quartz–pyrite±sphalerite–galena	Sericite±quartz±pyrite	2–10 mm; parallel margins; wide selvages	Sericite–chlorite and quartz–sericite–pyrite	Throughout the deposit, with sphalerite/galena common on margins of deposit into wallrock	D type
Anhydrite	None	Grey, white or pink; 1 mm to >1 m; recessively weathered, alter to gypsum	Anhydrite	Late stage, overprinting quartz-stockwork zones in core of deposit, and above core to surface, where they are mainly altered to gypsum	-
Quartz–bornite–tennantite/enargite	Quartz–pyrophyllite/dickite	5–40 mm; crackle sulphides within quartz veins	High sulphidation	Overprinting quartz-stockwork zones in centre of deposit	-

<sup>1</sup> Sillitoe (2010), modified from Gustafson & Hunt (1975)

shallower areas of the deposit, where they alter to gypsum (Table 2).

### Mineralization

Mineralization at the Kerr and Deep Kerr deposits is present as disseminations and within veins as fine-grained hypogene chalcopyrite, bornite, molybdenite and pyrite, with the occurrence of gold and silver intimately associated with sulphide mineralization (M. Savell, pers. comm., 2015). Mineralization is controlled by permeability, and is therefore more homogeneous within deeper, intrusion-hosted portions of the system and more erratic in shallower, mixed sedimentary, volcanic, and intrusion-hosted portions of the deposit. Mineralization is associated with early K-feldspar, chlorite and magnetite alteration, although later mineralization, such as evidenced by the high-sulphidation overprint of earlier stockworks, may have locally enriched metal grades.

### Discussion

To characterize the spatial and temporal distribution of alteration and mineralization, and their relation to hostrock lithology, fieldwork focused on relogging more than 7000 m of core on a cross-section across northern Kerr/Deep Kerr. Crosscutting relationships were utilized to develop a vein paragenesis, and will be corroborated with results from sulphur-isotope and petrographic analyses. Sulphur-isotope analyses will also substantiate correlation of

alteration assemblages with vein types and validate timing, such as the high-sulphidation overprint of quartz-stockwork zones. Field observations, such as the link between sedimentary rocks and yellow sericite alteration, and remnant K-feldspar–magnetite–chlorite alteration, will be characterized by whole-rock geochemistry, petrography and SWIR analysis. Samples collected for whole-rock geochemistry and petrographic analysis will be utilized for characterization of hosting rock types and alteration assemblages, which will aid in identification of altered hostrocks within the deposit. The more than 1100 chip samples collected will be utilized for SWIR analysis, which will be used in conjunction with geochemistry, petrography and field observations to produce a cross-sectional alteration model. The SWIR analysis will be verified through in-depth analyses by SEM, XRD and EPMA to provide confidence in this method as a rapid and reliable exploration tool.

The combination of these methods will enable the development of a hydrothermal-alteration cross-sectional model for the Kerr and Deep Kerr deposits that encompasses the spatial and temporal evolution of the ore system. It is anticipated that the results will provide a foundation for a better understanding of the complex hydrothermal alteration associated with porphyry deposits and lead to improved exploration success and geometallurgical decision making, both in British Columbia and in other porphyry districts.



## Acknowledgments

This research is being undertaken at the Mineral Deposit Research Unit at the University of British Columbia, in collaboration with Seabridge Gold Inc. Geoscience BC is acknowledged and thanked for the scholarship provided to

the first author to support efforts toward this project. The support and thoughtful help from M. Savell, W. Threlkeld and the rest of the team at Seabridge Gold is greatly appreciated, especially all those who helped move the kilometres of core required for this project. The review of this paper by G. Febbo is gratefully acknowledged.

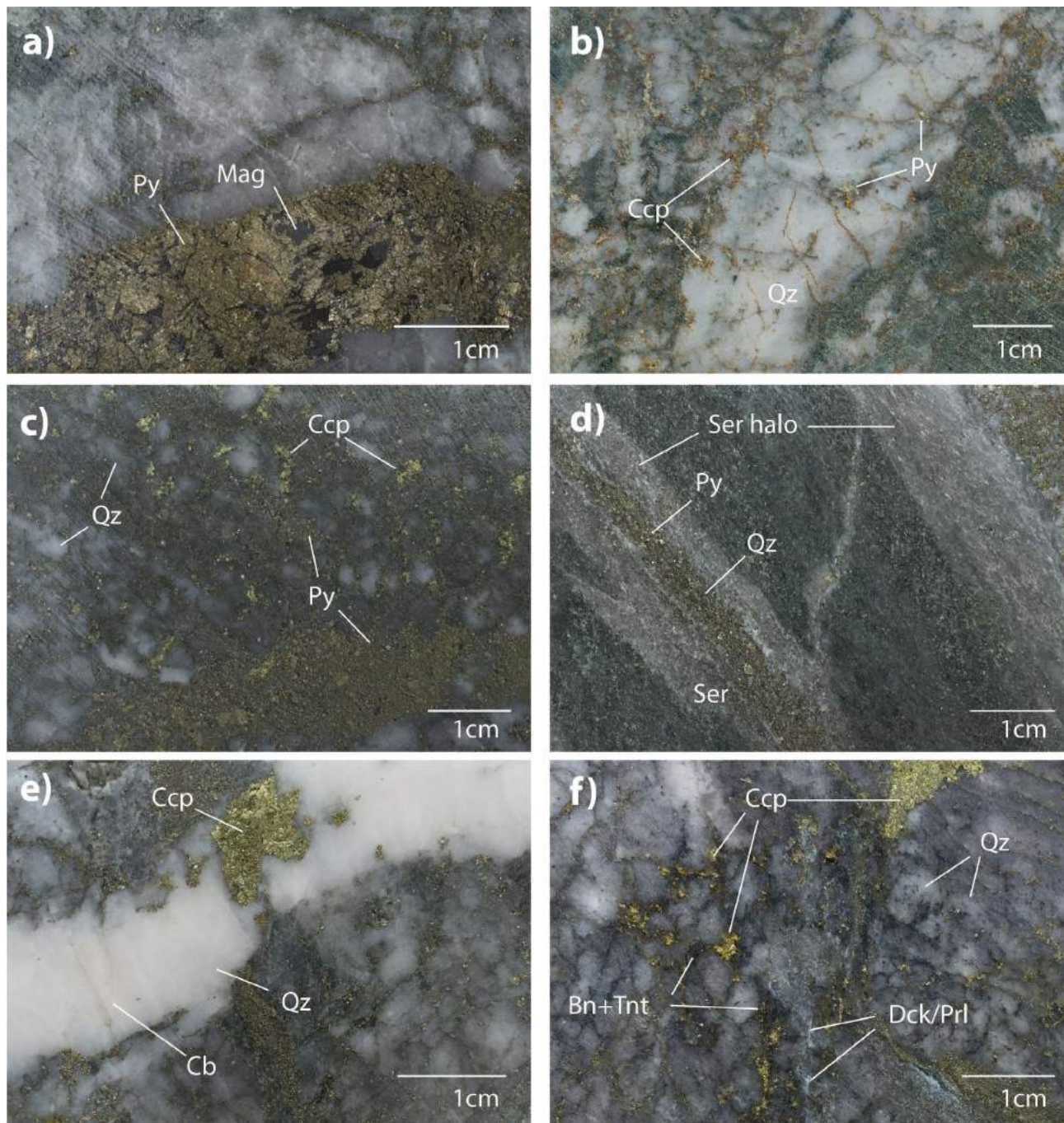


**Figure 6.** Overview of vein types at the Kerr and Deep Kerr deposits (drillhole number, depth in metres): **a)** magnetite-pyrite vein with alteration of magnetite to pyrite (K-13-32, 635 m); **b)** early granular milky quartz-chalcopyrite-pyrite A-type vein (K-13-34, 483.4 m); **c)** quartz-chalcopyrite-pyrite stockwork veining in core of deposit (K-13-31, 590 m); **d)** quartz-pyrite vein with wide sericite halo overprinting chlorite-sericite alteration (K-13-30, 749.6 m); **e)** late white quartz-chalcopyrite-carbonate vein (K-13-30, 598.6 m); **f)** high-sulphidation bornite-tennantite±dickite/pyrophyllite overprint of quartz stockwork with chalcopyrite in core of deposit (K-13-30, 567.2 m). Abbreviations: Bn, bornite; Cb, carbonate; Ccp, chalcopyrite; Chl, chlorite; Dck, dickite; Mag, magnetite; Prl, pyrophyllite; Py, pyrite; Qz, quartz; Ser, sericite; Tnt, tennantite.

## References

- Alldrick, D.J. and Britton, J.M. (1991): Sulphurets area geology; BC Ministry of Energy and Mines, BC Geological Survey, Open File 1991-21, scale 1:20 000.
- Bridge, D.J. (1993): The deformed Early Jurassic Kerr copper-gold porphyry deposit, Sulphurets gold camp, northwestern British Columbia; M.Sc. thesis, University of British Columbia, 319 p.
- Cohen, J.F. (2012): Compositional variation in hydrothermal white mica and chlorite from wall-rock alteration at the Ann-Mason porphyry copper deposit, Nevada; M.Sc. thesis, Oregon State University, 138 p.
- Dilles, J.H. (2012): Footprints of porphyry Cu deposits vectors to the hydrothermal center using mineral mapping and litho-geochemistry; final technical report for USGS MRERP Grant Award G10AP00052, Oregon State University, 599 p., URL <<http://minerals.er.usgs.gov/mrerp/reports/Dilles-G10AP00052.pdf>> [November 2015].
- Ditson, G.M., Wells, R.C. and Bridge, D.J. (1995): Kerr: the geology and evolution of a deformed porphyry copper-gold deposit, northwestern British Columbia; *in* Porphyry Deposits of the Northwestern Cordillera of North America, T.G. Schroeter (ed.), Canadian Institute of Mining, Metallurgy and Petroleum, Special Volume 46, p. 509–523.
- Febbo, G.E., Kennedy, L.A., Savell, M., Creaser, R.A. and Friedman, R.M. (2015): Geology of the Mitchell Au-Cu-Ag-Mo porphyry deposit, northwestern British Columbia, Canada; *in* Geological Fieldwork 2014, BC Ministry of Energy and Mines, BC Geological Survey, Paper 2015-1, p. 59–86, URL <[http://www.empr.gov.bc.ca/Mining/Geoscience/PublicationsCatalogue/Fieldwork/Documents/2014/04\\_Febbo\\_etal.pdf](http://www.empr.gov.bc.ca/Mining/Geoscience/PublicationsCatalogue/Fieldwork/Documents/2014/04_Febbo_etal.pdf)> [October 2015].
- Febbo, G.F., Freeman, J., Kraft, T. and Kennedy, L.A. (2014): Geology of the KSM property: waste rock characterization; in-house geology map for Seabridge Gold Inc.
- Gustafson, L.B. and Hunt, J.P. (1975): The porphyry copper deposit at El Salvador, Chile; *Economic Geology*, v. 90, p. 2–16.
- Jimenez, T.R.A. (2011): Variation in hydrothermal muscovite and chlorite composition in the Highland Valley porphyry Cu-Mo district, British Columbia, Canada; M.Sc. thesis, University of British Columbia, 249 p.
- Kirkham, R.V. (1963): The geology and mineral deposits in the vicinity of the Mitchell and Sulphurets glaciers, northwest British Columbia; M.Sc. thesis, University of British Columbia, 142 p.
- Kirkham, R.V. and Margolis, J. (1995): Overview of the Sulphurets area, northwestern British Columbia; *in* Porphyry Deposits of the Northwestern Cordillera of North America, T.G. Schroeter (ed.), Canadian Institute of Mining, Metallurgy and Petroleum, Special Volume 46, p. 473–483.
- Kyba, J. (2014): The Stuhini-Hazelton unconformity of Stikinia: investigations at KSM-Brucejack, Snip-Johnny Mountain and Red Chris areas (abstract); 2014 Geological Society of America Annual Meeting, Vancouver, BC, October 19–22, 2014, Abstracts with Programs, v. 46, no. 6, p. 589, URL <<https://gsa.confex.com/gsa/2014AM/webprogram/Paper248935.html>> [October 2015].
- Lewis, P.D. (2001): Geological maps of the Iskut River area; *in* Metallogenesis of the Iskut River Area, Northwestern British Columbia, P.D. Lewis, A. Toma and R.M. Tosdal (ed.), University of British Columbia, Mineral Deposit Research Unit, Special Publication 1, p. 77–83.
- Logan, J.M. and Mihalynuk, M.G. (2014): Tectonic controls on Early Mesozoic paired alkaline porphyry deposit belts (Cu-Au±Ag-Pt-Pd-Mo) within the Canadian Cordillera; *Economic Geology*, v. 109, p. 827–858.
- Logan, J.M., Drobe, J.R. and McClelland, W.C. (2000): Geology of the Forrest Kerr–Mess Creek area, northwest British Columbia (NTS 104B/10, 15 and 104/G2, 7W); BC Ministry of Energy and Mines, BC Geological Survey, Bulletin 104, 163 p., URL <<http://www.empr.gov.bc.ca/mining/geoscience/publicationscatalogue/bulletininformation/bulletinsafter1940/Pages/Bulletin104.aspx>> [October 2015].
- Margolis, J. (1993): Geology and intrusion-related copper-gold mineralization, Sulphurets, British Columbia; Ph.D. thesis, University of Oregon, 289 p.
- Nelson, J. and Kyba, J. (2014): Structural and stratigraphic control of porphyry and related mineralization in the Treaty Glacier–KSM–Brucejack–Stewart trend of western Stikinia; *in* Geological Fieldwork 2013, BC Ministry of Energy and Mines, BC Geological Survey, Paper 2014-1, p. 111–140, URL <[http://www.empr.gov.bc.ca/Mining/Geoscience/PublicationsCatalogue/Fieldwork/Documents/2013/07\\_Nelson\\_Kyba.pdf](http://www.empr.gov.bc.ca/Mining/Geoscience/PublicationsCatalogue/Fieldwork/Documents/2013/07_Nelson_Kyba.pdf)> [October 2015].
- Panteleyev, A. (1995): Porphyry Cu±Mo±Au; *in* Selected British Columbia Mineral Deposit Profiles, D.V. Lefebure and G.E. Ray (ed.), BC Ministry of Energy and Mines, BC Geological Survey, Open File 1995-20, p. 87–92, URL <<http://www.empr.gov.bc.ca/mining/geoscience/mineraldepositprofiles/listbydepositgroup/pages/lporphyry.aspx#104>> [September 2015].
- Seabridge Gold Inc. (2015a): Mineral reserves and resources (updated March 26, 2015); Seabridge Gold Inc., URL <<http://seabridgegold.net/resources.php>> [December 2015].
- Seabridge Gold Inc. (2015b): Seabridge Gold reports 52% resource expansion for KSM’s Deep Kerr deposit; Seabridge Gold Inc., press release, March 23, 2015, URL <<http://seabridgegold.net/News/Article/516/seabridge-gold-reports-52%25-resource-expansion-for-ksm-s-deep-kerr-deposit-estimated-782-million-tonne-inferred-resource-averages-0.54%25-copper-and-0.33-g-t-gold.-deposit-now-contains-estimated-8.2-million-ounces-gold>> [December 2015].
- Sillitoe, R.H. (2010): Porphyry copper systems; *Economic Geology*, v. 105, p. 3–41.
- Wilson, A.J., Cooke, D.R., Harper, B.J. and Deyell, C.L. (2007): Sulfur isotopic zonation in the Cadia district, southeastern Australia: exploration significance and implications for the genesis of alkalic porphyry gold-copper deposits; *Mineralium Deposita*, v. 42, p. 465–487.